Journal of Radiation Research, 2013, 54, 260–267
doi: 10.1093/jrr/rrs102 Advance Access Publication 6 November 2012

Effect of bevacizumab treatment on *p*-boronophenylalanine distribution in murine tumor

Yong LIU[1,†], Minoru SUZUKI[2], Shin-ichiro MASUNAGA[2], Yi-Wei CHEN[3], Genro KASHINO[4], Hiroki TANAKA[2], Yoshinori SAKURAI[2], Mitsunori KIRIHATA[5] and Koji ONO[2,*]

[1]Department of Radiation Oncology, Fudan University Shanghai Cancer Center, Department of Oncology, Shanghai Medical College, Fudan University, Shanghai 200032, PR China
[2]Research Reactor Institute, Kyoto University, Osaka 590-0494, Japan
[3]Department of Radiation Oncology, Taipei Veterans General Hospital, Taipei 112, Taiwan
[4]Oita University, Faculty of Medicine, Hazama-cho, Yufu-city, Oita 879-5593, Japan
[5]Graduate School of Life and Environmental Sciences, Osaka Prefecture University, Sakai-city 599-8531, Japan
*Corresponding author. Tel: +81-72-451-2475; Fax: +81-72-451-2627; E-mail: onokoji@rri.kyoto-u.ac.jp
[†]Previous Affiliation: Research Reactor Institute, Kyoto University, Japan

(Received 18 April 2012; revised 20 September 2012; accepted 5 October 2012)

Previous studies have demonstrated that angiogenesis inhibitors can enhance tumor inhibitory effects of chemo- and radiotherapy via their action on tumor vessels. Here, we studied the effect of the angiogenesis inhibitor, bevacizumab (Avastin), on boron distribution in a murine tumor model. The human head and neck squamous cell carcinoma cell line was used for inoculation into mice. Boron-10 concentrations in tissues were measured by prompt γ-ray spectrometry (PGA). Hoechst 33342 perfusion and *p*-boronophenylalanine (BPA) distribution were determined by immunofluorescence staining. Our results revealed enhanced tumor blood perfusion and BPA accumulation in tumors after Avastin treatment, suggesting that combination of angiogenesis inhibition with treatment with boron compound administration may improve the efficacy of boron neutron capture therapy (BNCT) by modifying tumor vessels. In addition, our results also demonstrated the usefulness of immunofluorescence staining for investigating boron compound distribution at the cellular level.

Keywords: angiogenesis inhibitor; bevacizumab; boron compounds; BNCT

INTRODUCTION

The advantages of boron neutron capture therapy (BNCT) have been demonstrated in the treatment of malignant glioblastomas, melanomas and other cancers because of its selective destruction of tumor cells [1–3]. In essence, a non-cytotoxic boron compound is selectively enriched in tumor cells. During the subsequent irradiation of thermal neutrons, ^{10}B captures thermal neutrons and emits high-energy α and lithium (^{7}Li) particles with an energy level of 2.79 MeV and paths ≤10 μm. Since the path length is approximately the size of a cell, it destroys tumor cells selectively without affecting the surrounding normal tissues [4].

BNCT is a binary treatment modality based on the reaction between a stable boron isotope and thermal neutrons. Its efficacy is primarily dependent on boron compound distribution in tumor cells. However, the abnormal structure and function of tumor vessels leads to a decreased uptake of the boron compound into tumors [5]. Thus, the regulation of tumor vessels and improvement of blood perfusion is important for increasing the uptake of the boron compound into tumors.

Bevacizumab (Avastin), the first anti-vascular endothelial growth factor (VEGF) agent, is a recombinant humanized monoclonal antibody to VEGF [6]. VEGF is over-expressed in tumors, and contributes to angiogenesis, tumor growth and metastasis [7]. In clinical trials, Avastin has been shown to improve the efficacy of both chemo- and radiotherapy [8, 9]. It acts by normalizing tumor vessels, thus increasing drug and oxygen delivery to the tumor, thereby contributing to tumor inhibition induced by chemo- and radiotherapy [10]. Here, we investigated the effects of

Avastin on boron compound distribution in a mouse model of the human head and neck squamous cell carcinoma.

MATERIALS AND METHODS

Cell lines and culture conditions

The human head and neck squamous cell carcinoma cell line SAS (SAS/neo, transfected with neo vector), was cultured in Dulbecco's modified Eagle's medium (Sigma-Aldrich Co. LLC, St. Louis, MO, USA) supplemented with 10% fetal bovine serum, and maintained at 37°C in an atmosphere of 95% air and 5% CO_2.

Animals and tumor model

Female BALB/C nu-nu mice, aged 6 weeks, were purchased from Japan Animal Co., Ltd, Osaka, Japan. The animals were housed in a pathogen-free room under controlled conditions of temperature, humidity, and a 12-hour dark/light cycle, and acclimatized for 1 week before tumor cell transplantation. SAS cells (1×10^5) cells were inoculated subcutaneously into the hind legs of the 7-week-old BALB/C nude mice. Fourteen days after cell inoculation, the tumor had reached approximately 10 mm in diameter. Tumor volume was calculated using the following formula: $V = \pi/6 \times a \times b^2$, where a and b are the longest and shortest diameters of the tumors, respectively. All animal experiments were carried out in accordance with the Guidelines for Handling of Laboratory Animals for Biomedical Research, compiled by the Committee on Safety Handling Regulations for Laboratory Animal Experiments, Kyoto University.

Treatment with the boron compound and bevacizumab

The boron-10 compound, *p*-boronophenylalanine (BPA), was purchased from Boron Biologicals, Inc. (Raleigh, NC, USA) and an aqueous solution of BPA (24.2 mg/ml, ^{10}B: 1300 mg/l) was prepared. Bevacizumab (Avastin, 21900AMX00921) was purchased from CHUGAI Pharmaceutical Co., Ltd (Tokyo, Japan). For *in vitro* experiments, SAS cells were incubated with the BPA solution at different ^{10}B concentrations (0, 0.65, 1.3, 3.9, 7.8, 15.6 and 31.2 ppm) (1 ppm = 1 mg/l) for 1 h. For *in vivo* experiments, mice received a single-dose intraperitoneal injection (i.p.) of Avastin [125, 250 and 375 μg/25 g body weight (BW)], and the tumors were excised 0.5–7 days later. BPA (250 mg/kg BW) was administered by i.p. injection 1 h before tumor excision.

Tumor blood perfusion and histological analysis

In brief, Hoechst 33342 (16 mg/kg) was injected via the tail vein 1 min before tumor excision. The tumors samples were flash-frozen in liquid nitrogen. Five-micrometer-thick slices of tumor sections were cut and mounted on glass-slides using 50% glycerol containing propidium iodide (PI). Hematoxylin–eosin (HE) staining was used for histological analysis.

Immunofluorescence staining for examining BPA distribution

SAS cells were cultured on cover glass at a concentration of 5×10^5 cells per well in six-well plates. One hour after incubation with the BPA solution, the cells were washed with phosphate buffer solution (PBS) and immediately fixed with a 4% formaldehyde buffer solution for 20 min at 4°C. The cells were then permeabilized with 0.2% Triton X-100 for 15 min and blocked with 1% bovine serum albumin (BSA) in PBS for 60 min at room temperature. The cells were then incubated with a BPA monoclonal antibody [11] (10 μg/ml) (supplied by Dr Mitsunori Kirihata, Osaka Prefecture University, Japan) for 1 h at room temperature, washed three times in PBS, and then incubated with Alexa Fluor 594 labeling antibody (1:400) (Molecular Probes, Eugene, OR, USA) for 1 h in the dark. Cells were then mounted on slides using 50% glycerol with 4,6-diamino-2-phenylindole (DAPI) (1:500). Normal serum was used instead of primary antibodies as a negative control.

The tumor tissue obtained was flash-frozen with liquid nitrogen after treatment with BPA or Avastin. Five-micrometer-thick sections of the tumor were cut and processed for immunofluorescence staining as mentioned above for the cultured SAS cells.

All images were obtained using a fluorescence microscope (BZ-9000, KEYENCE, Japan).

Quantitative analysis of BPA distribution in cells

For quantitative analysis, the BPA distribution in cells was measured as an immunofluorescence intensity number. Absorption/emission wavelengths of 590/617 nm were used for measuring Alexa Fluor 594 fluorescence. Briefly, cells were selected from the images obtained, and the immunofluorescence intensity per cell was measured for every cell. A total of 300–500 cells were tested for each experiment, using Adobe Photoshop (Adobe Systems, San Jose, CA, USA).

Measurement of boron-10 concentration in tissues

The tumors and surrounding normal muscle tissues were obtained after BPA administration, and the ^{10}B concentrations were measured by prompt γ-ray (PGA) spectrometry using a thermal neutron guide tube at Kyoto University Research Reactor Institute.

Double immunofluorescence staining of tumor vessels

Briefly, frozen tumor tissue sections were fixed with 4% formaldehyde buffer solution for 20 min at 4°C. The slices were then permeabilized with 0.2% Triton X-100

for 15 min, blocked with 1% BSA in PBS for 60 min at room temperature, and then incubated with a 1:200 dilution of goat anti-PECAM1(CD31) polyclonal antibody (Santa Cruz Biotechnology, Santa Cruz, CA, USA) and rabbit anti-collagen IV polyclonal antibody (Abcam, Cambridge, MA, USA) overnight at 4°C. The slides were then washed in PBS and incubated with 1:1000 dilution, tetramethylrhodamine-5(and-6)-isothiocyanate (TRITC)-conjugated rabbit F(ab,)2 fragment to goat IgG (MP Biomedicals, Solon, OH, USA) and FITC-conjugated goat affinity purified IgG against rabbit IgG (MP Biomedicals, Solon, OH, USA). Immunofluorescence staining was observed using a fluorescence microscope (BZ-9000, KEYENCE, Japan).

For quantitative analysis of blood perfusion and tumor vessels in tumor tissues, the levels of Hoechst perfusion and CD31 staining were measured as blue and red pixel numbers using Adobe Photoshop, according to the analytical digital photomicroscopy (ADP) technique [12]. Briefly, the brightness and contrast of each image was adjusted, the best blue or red range for all images was chosen, and the pixel number of each was recorded.

Statistical analysis

All experiments were repeated four to six times. Data are presented as mean ± standard deviation. Statistical analyses were performed using Student's *t*-test with KaleidaGraph

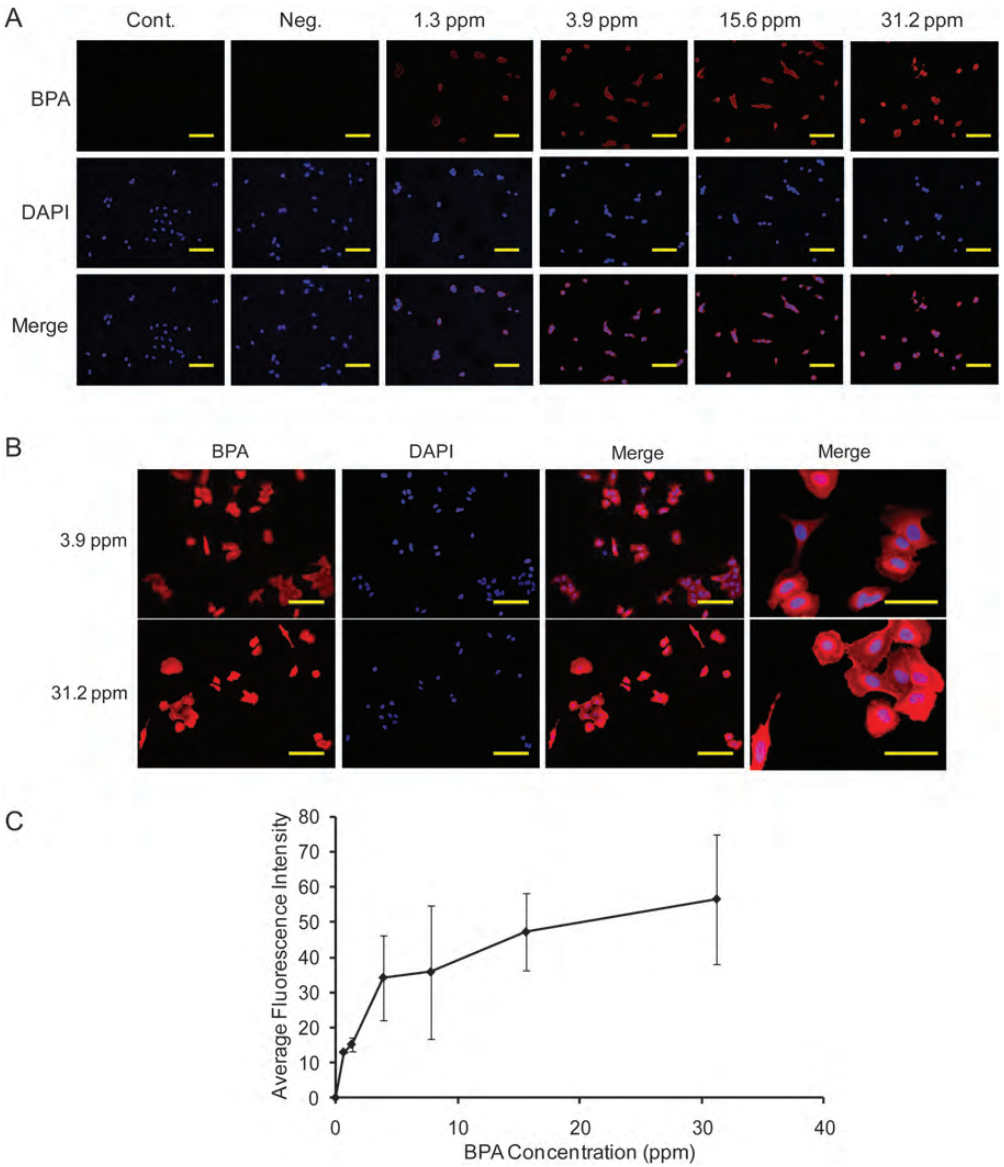

Fig. 1. Representative immunofluorescence staining of BPA (**A**, **B**) and average BPA distribution in SAS cells (**C**). Cont: cells treated with PBS. Bars represent 50 μm.

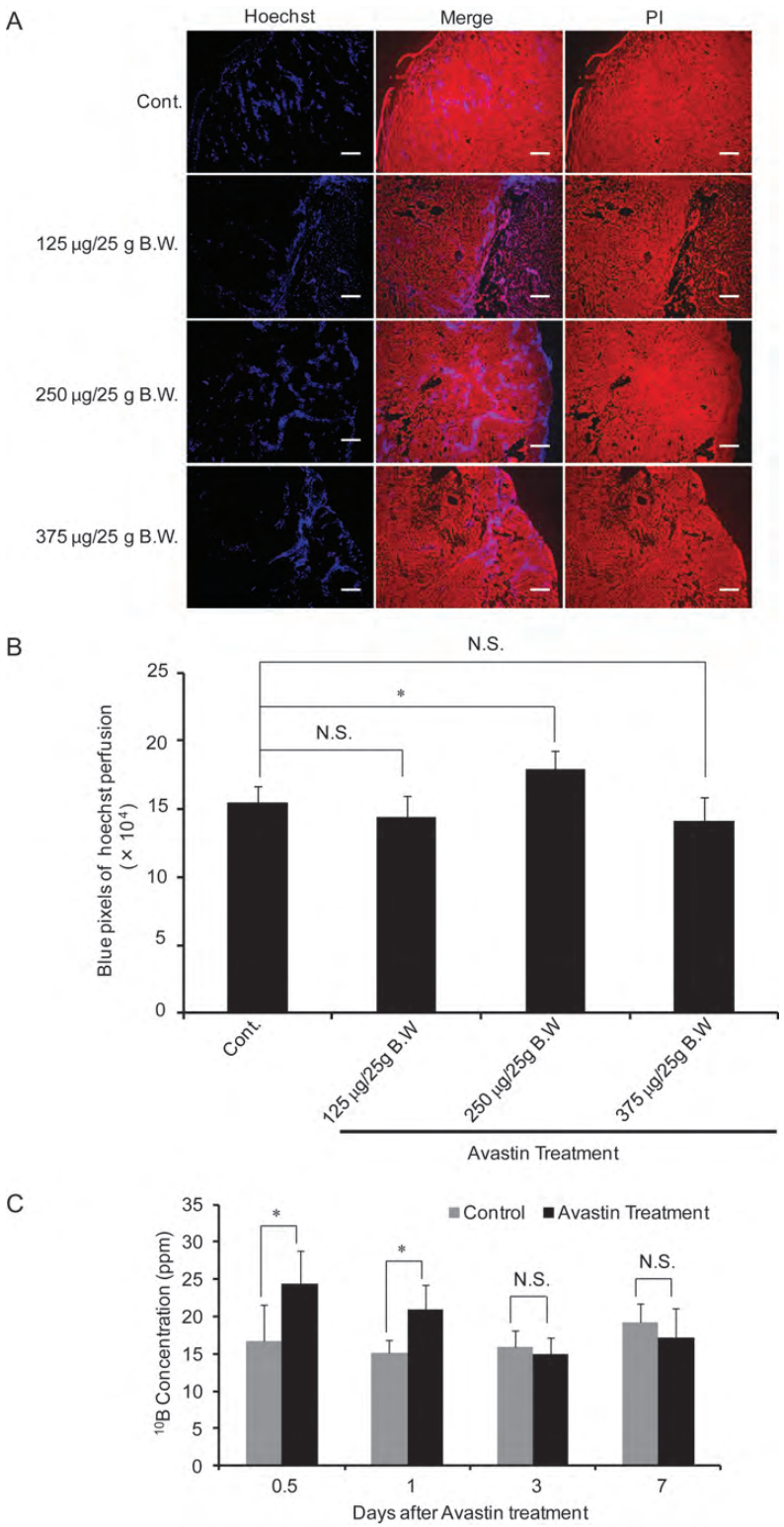

Fig. 2. Effect of Avastin treatment on tumor blood perfusion. Representative immunofluorescence staining of Hoechst 33342 (**A**), and quantitative analysis of Hoechst 33342 (**B**) after treatment with increasing concentrations of Avastin for 1 day. Time-dependent boron concentration in mice tumors treated with Avastin (250 μg/25 g BW) (**C**). Bars represent 50 μm. $^{*}P < 0.05$, NS: not significant.

(Version 4.0, Synergy Software). P values < 0.05 were considered statistically significant.

RESULTS

BPA distribution in SAS cells

The BPA distribution in SAS cells was analyzed by immunofluorescence staining. The results showed that BPA accumulated specifically around the nucleus of the cells (Fig. 1A, B). No immunofluorescence staining was observed in the non-treated control cells. The average distribution of BPA in SAS cells was determined by immunofluorescence intensity 1 h after BPA treatment. The immunofluorescence intensity of BPA staining increased with increasing concentrations of ^{10}B up to 31.2 ppm in SAS cells; the intensity of BPA staining increased in a dose-dependent manner (Fig. 1C).

Effect of Avastin treatment on BPA distribution in tumors

The effect of Avastin on blood perfusion in tumors was investigated by Hoechst 33342 perfusion, 1 day after Avastin treatment at doses of 125, 250 or 375 μg/25 g BW. Avastin treatment at a dose of 250 μg/25 g BW. significantly increased blood perfusion as compared with control mice treated by saline instead of Avastin. However, a significant change in Hoechst 33342 perfusion was not found after treatment with 125 μg/25 g BW and 375 μg/25 g BW compared with control mice treated by saline instead of Avastin (Fig. 2A, B).

To study the time-dependent effect of Avastin on BPA distribution in tumors, we analyzed ^{10}B concentrations 0.5–7 days after administration of 250 μg/25 g BW. Avastin. The concentration of ^{10}B in tumors increased significantly from 0.5–1 day after Avastin treatment as compared with the saline-treated control mice, and then decreased to the control level, 3 days after Avastin treatment (Fig. 2C).

Effect of Avastin treatment on tumor volume

Immunofluorescence staining showed improved BPA distribution in tumor tissues 1 day after Avastin treatment (250 μg/25 g B.W). as compared with the saline-treated control mice (Fig. 3A). However, a significant difference in tumor volume was not found from 0.5–7 days as compared with the controls (Fig. 3B).

Effect of Avastin treatment on tumor vessels

The effect of Avastin on tumor vessels was analyzed by immunofluorescence staining with antibodies against CD31 and collagen IV. As shown in Fig. 4A, CD31 and collagen IV expression decreased 1 day after Avastin treatment (250/25°g BW) as compared with the control mice. In addition, the colocalized region appeared more normalized after

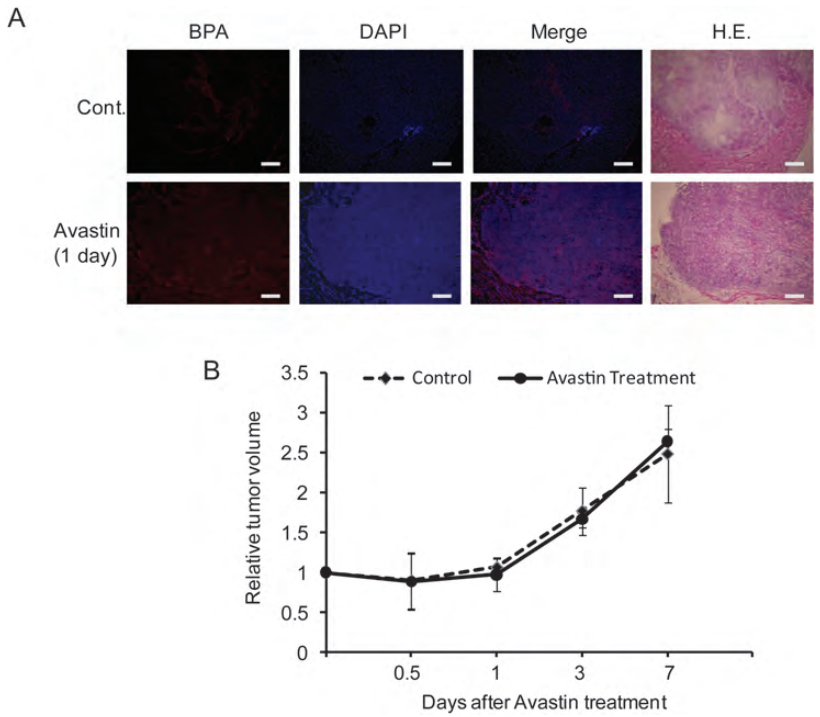

Fig. 3. Effect of Avastin treatment on tumor BPA distribution and tumor volume. Representative immunofluorescence staining of BPA distribution (**A**) and volume of SAS tumors (**B**). Cont: mice treated with saline. BPA treatment: 250 μg/25 g BW for 1 day. Bars represent 50 μm.

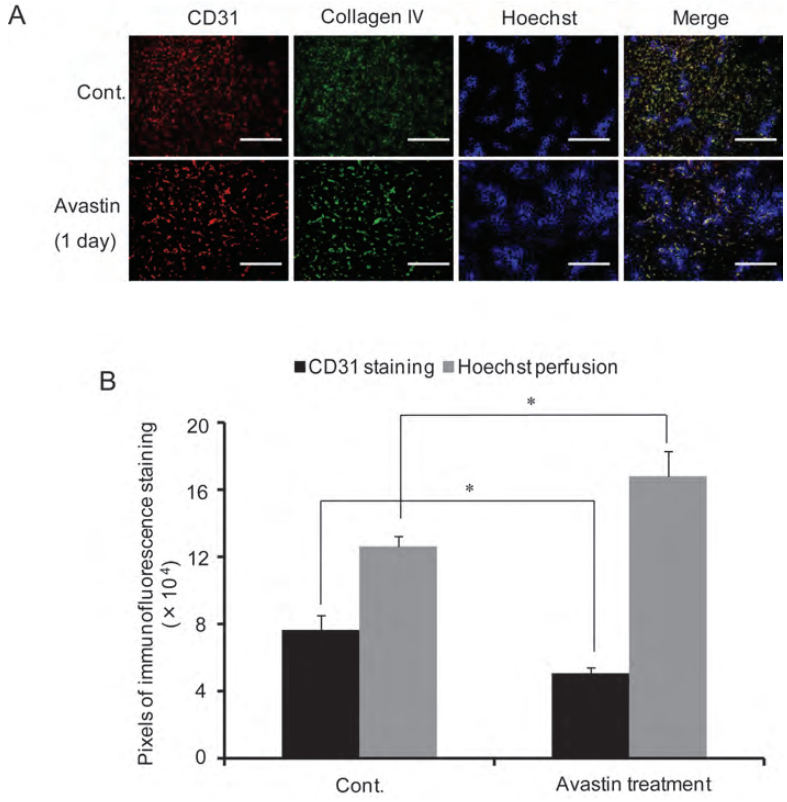

Fig. 4. Effect of Avastin treatment on tumor vessels. Representative images of CD31, Collagen IV and Hoechst 33342 distribution (**A**), quantitative analysis of CD31 and Hoechst 33342 (**B**) after Avastin treatment at a dose of 250 μg/25 g BW for 1 day. Cont: saline-treated mice. Bars represent 50 μm. *$P < 0.05$.

Avastin treatment. In addition, Hoechst distribution in Avastin-treated mice was significantly greater as compared with that of control mice, with decreased CD31 staining (Fig. 4B).

DISCUSSION

The use of BNCT for cancer treatment has become popular due to its successful use in the treatment of melanomas and other malignant tumors [13, 14]. BNCT is a tumor cell-targeted radiation therapy, based on the highly selective distribution of boron compound in tumor cells [15]. The delivery of boron into tumors is considered to be the key to the success of BNCT [16, 17]. Tumor vessels are abnormal in structure and function differently from the normal vasculature, which leads to insufficient delivery of oxygen and drugs [18, 19]. Thus, improving the blood supply to tumors as well as normalization of tumor vasculature might be more important to BNCT treatment.

Tumor growth, invasion and subsequent metastasis depend on an adequate blood supply through the process of angiogenesis [20]. VEGF is a key pro-angiogenesis factor and can be produced by a variety of cells, including tumor cells, which promote invasion and migration of endothelial cells, thus contributing to tumor growth and metastasis to distant sites. Avastin is a humanized monoclonal antibody, which can bind soluble VEGF and inhibit the interaction of VEGF with its receptors on the surface of endothelial cells, thereby neutralizing its activity. Anti-angiogenesis therapy is designed to destroy or block the function of tumor-associated vessels in order to deprive the tumor cells of oxygen and nutrients, thereby inhibiting tumor growth [21, 22]. However, the efficacy of anti-angiogenesis therapy depends on the time and dose of administration. Jain *et al.* have suggested that VEGF inhibitors can increase tumor oxygen and drug delivery by modifying tumor vessels at a certain dose, which was named as the normalization window [10]. In the present study, our results showed that the Hoechst perfusion and ^{10}B concentration in tumors increased significantly 1 day after a 250-μg/25 g BW. Avastin dose. However, Hoechst tumor perfusion decreased at an Avastin dose of 375 μg/25 g BW, demonstrating the concentration-dependent effects of Avastin treatment in inhibiting tumor angiogenesis and reducing tumor blood

perfusion. In addition, we found that the ^{10}B concentration in the tumor cells increased significantly 1 day after Avastin treatment, but decreased from Day 3 after Avastin treatment, suggesting time-dependent effect of Avastin treatment on blood perfusion. These showed that the normalization of tumor vessels induced by Avastin treatment existed in a time and dose range. Blood perfusion in tumor can be improved in the normalization window. However, existing tumor vessels and angiogenesis were inhibited with increasing dose and duration of Avastin treatment by affecting VEGF signaling, which decreased the drug delivery and distribution into the tumor tissue [10].

Tumor blood perfusion generally decreased with increase in tumor volume due to a necrosis region. Although the ^{10}B concentration in cells and Hoechst distribution increased 1 day after Avastin treatment at a dose of 250 μg/25 g BW, a single dose of Avastin was not found to have an effect on tumor volume. In our previous study, bevacizumab (Avastin) treatment improved acute hypoxia in B16-BL6 melanoma [23]. The above results all suggested that Avastin treatment improves tumor blood perfusion. Further, studies have shown that following Avastin treatment, the viability of leaky and torturous tumor vessels decreased significantly, but vessels covered with collagen IV became larger and more robust. These results suggest that a single-dose Avastin treatment (250 μg/25 g BW) enhances boron compound distribution in tumors by modifying tumor vessel structure and improving tumor blood perfusion, but does not cause tumor volume inhibition. In addition, in some tumor vessels, the collocation of Hoechst perfusion with CD31 was not evident after Avastin treatment, suggesting that some tumor vessels might be impervious to the Avastin treatment. Tumor vessel normalization induced by other angiogenesis inhibitors, including Anginex and thalidomide [24, 25], has also been shown to improve the efficacy of traditional radiation treatment and BNCT. The pharmacologically (VEGF inhibitors) induced normalization is transient, characterized by a time window of 1–2 days after treatment, and is concentration dependent. Studies have demonstrated Rgs5 (regulator of G protein signaling 5), Ang-1, 2 (angiopoietin-1, 2) and PHD2 (HIF-prolyl hydroxylases 2) to be directly implicated in the development of abnormal tumor vessel formation and normalization in a VEGF-independent manner [26–28].

PGA and ICP are currently employed techniques, but could not be used to evaluate the cellular distribution of boron in tumor tissues and cancer cells in detail. In this study, we investigated boron compound distribution in cells by immunofluorescence staining using an antibody designed for the boron compound. Our results demonstrated that immunofluorescence staining is specifically effective for investigating the delivery of boron.

In summary, our studies demonstrated that Avastin treatment, when used at a suitable dose and for a specific time frame, can improve boron compound distribution in tumor tissues. In addition, immunofluorescence staining of boron compound is effective in evaluating the boron compound distribution at the cellular level. Further investigation regarding the structure and function of tumor vasculature structure may be necessary to enhance the effects of BNCT treatment.

ACKNOWLEDGEMENTS

The authors are grateful to Mrs Masami Fukui for her technical assistance during the study. This research was supported by a Grant-in-Aid for Scientific Research for Young Scientists (22791188) from the Japan Ministry of Education, Science, Sports and Culture to Y. Liu, a Grant-in-Aid 2010 (No. 53) from the Japan Radiation Effects Association to Y. Liu, and a Grant-in-Aid 2010 from the Japan Osaka Cancer Society to Y. Liu.

REFERENCES

1. Pisarev MA, Dagrosa MA, Juvenal GJ. Boron neutron capture therapy in cancer: past, present and future. *Arq Bras Endocrinol Metabol* 2007;**51**:852–6.
2. Kageji T, Mizobuchi Y, Nagahiro S *et al*. Clinical results of boron neutron capture therapy (BNCT) for glioblastoma. *Appl Radiat Isot* 2011;**69**:1823–5.
3. Kageji T, Mizobuchi Y, Nagahiro S *et al*. Long-survivors of glioblatoma treated with boron neutron capture therapy (BNCT). *Appl Radiat Isot* 2011;**69**:1800–2.
4. Coderre JA, Turcotte JC, Riley KJ *et al*. Boron neutron capture therapy: cellular targeting of high linear energy transfer radiation. *Technol Cancer Res Treat* 2003;**2**:355–75.
5. De Bock K, Cauwenberghs S, Carmeliet P. Vessel abnormalization: another hallmark of cancer? Molecular mechanisms therapeutic implications. *Curr Opin Genet Dev* 2011;**21**: 73–9.
6. Shih T, Lindley C. Bevacizumab: an angiogenesis inhibitor for the treatment of solid malignancies. *Clin Ther* 2006;**28**:1779–802.
7. Waldner MJ, Neurath MF. Targeting the VEGF signaling pathway in cancer therapy. *Expert Opin Ther Targets* 2012;**16**: 5–13.
8. Ferrara N, Hillan KJ, Novotny W. Bevacizumab (Avastin), a humanized anti-VEGF monoclonal antibody for cancer therapy. *Biochem Biophys Res Commun* 2005;**333**:328–35.
9. Ranieri G, Patruno R, Ruggieri E *et al*. Vascular endothelial growth factor (VEGF) as a target of bevacizumab in cancer: from the biology to the clinic. *Curr Med Chem* 2006;**13**: 1845–57.
10. Fukumura D, Jain RK. Tumor microvasculature and microenvironment: targets for anti-angiogenesis and normalization. *Microvasc Res* 2007;**74**:72–84.
11. Inoue N, Kusumoto M, Nakazawa M *et al*. The making of BPA monoclonal antibody and the analysis of its primary structure. *The program of the 4th meeting of Japan boron neutron capture therapy*. 2007;**23**.

12. Tabata C, Kadokawa Y, Tabata R *et al*. All-transretinoic acid prevents radiation- or bleomycin-induced pulmonary fibrosis. *Am J Repair Crit Care Med* 2006;**174**:1352–60.
13. Yamamoto T, Nakai K, Matsumura A. Boron neutron capture therapy for glioblastoma. *Cancer Lett* 2008;**262**:143–52.
14. Kato I, Fujita Y, Maruhashi A *et al*. Effectiveness of boron neutron capture therapy for recurrent head and neck malignancies. *Appl Radiat Isot* 2009;**67**:S37–42.
15. Barth RF. Boron neutron capture therapy at the crossroads: challenges and opportunities. *Appl Radiat Isot* 2009;**67**:S3–6.
16. Kumar S, Freytag SO, Barton KN *et al*. A novel method of boron delivery using sodium iodide symporter for boron neutron capture therapy. *J Radiat Res* 2010;**51**:621–6.
17. Nakamura H. Liposomal boron delivery for neutron capture therapy. *Methods Enzymol* 2009;**465**:179–208.
18. Jain RK. Barriers to drug delivery in solid tumors. *Sci Am* 1994;**271**:58–65.
19. McDonald DM, Baluk P. Significance of blood vessel leakiness in cancer. *Cancer Res* 2002;**62**:5381–5.
20. Bikfalvi A, Moenner M, Javerzat S *et al*. Inhibition of angiogenesis and the angiogenesis/invasion shift. *Biochem Soc Trans* 2011;**39**:1560–4.
21. Shinkaruk S, Bayle M, Laïn G, Déléris G. Vascular endothelial cell growth factor (VEGF), an emerging target for cancer chemotherapy. *Curr Med Chem Anticancer Agents* 2003;**3**:95–117.
22. Pircher A, Hilbe W, Heidegger I *et al*. Biomarkers in tumor angiogenesis and anti-angiogenic therapy. *Int J Mol Sci* 2011;**12**: 7077–99.
23. Masunaga S, Liu Y, Tanaka H *et al*. Reducing intratumour acute hypoxia through bevacizumab treatment, referring to the response of quiescent tumour cells and metastatic potential. *Br J Radiol* 2011;**84**:1131–8.
24. Dings RP, Loren M, Heun H *et al*. Scheduling of radiation with angiogenesis inhibitors anginex and Avastin improves therapeutic outcome via vessel normalization. *Clin Cancer Res* 2007;**13**:3395–402.
25. Molinari AJ, Pozzi EC, Monti Hughes A *et al*. Tumor blood vessel 'normalization' improves the therapeutic efficacy of boron neutron capture therapy (BNCT) in experimental oral cancer. *Radiat Res* 2012;**177**:59–68.
26. Hamzah J, Jugold M, Kiessling F *et al*. Vascular normalization in Rgs5-deficient tumours promotes immune destruction. *Nature* 2008;**453**:410–14.
27. Chae SS, Kamoun WS, Farrar CT *et al*. Angiopoietin-2 interferes with anti-VEGFR2-induced vessel normalization and survival benefit in mice bearing gliomas. *Clin Cancer Res* 2010;**16**:3618–27.
28. Kaelin WG, Jr, Ratcliffe PJ. Oxygen sensing by metazoans: the central role of the HIF hydroxylase pathway. *Mol Cell* 2008;**30**:393–402.